Research Paper
Computational Methods for Differential Equations
http://cmde.tabrizu.ac.ir
Vol. *, No. *, *, pp. 1-19
DOI:10.22034/cmde.2025.66080.3074

A numerical scheme with high accuracy to solve the two-dimensional time-space diffusion-wave model in terms of the Riemann-Liouville and Riesz fractional derivatives

Yadollah Ordokhani[1,*], **Mohammad Hossein Derakhshan**[1], **and Pushpendra Kumar**[2]

[1]Department of Mathematics, Faculty of Mathematical Sciences, Alzahra University, Tehran, Iran.

[2]Faculty of Engineering and Natural Sciences, Istanbul Okan University, Istanbul, Turkey.

Abstract

In this paper, we propose a hybrid and efficient numerical scheme with high accuracy to obtain approximate solutions of the two-dimensional time-space diffusion-wave model in terms of the Riemann-Liouville and Riesz fractional derivatives. To discretise the presented model, two approaches are used in the directions of space and time. In the time direction, we use a second-order accurate difference numerical method and the weighted shifted Grünwald derivative approximation of second-order. The weighted shifted Grünwald derivative approximation is used to estimate the Riemann–Liouville's fractional operator. Also, in the space direction, the Galerkin spectral method based on the modified Jacobi functions is used. The study of convergence and stability analysis for the proposed numerical approach is presented. At the end, some numerical examples are given to show the effectiveness of the proposed numerical scheme. For all the examples, graphs are drawn, and numerical results are reported in tables.

Keywords. Diffusion-wave model, Weakly singular kernel, Riesz fractional opertaor, Galerkin spectral method, Stability and convergence.
2010 Mathematics Subject Classification. 26A33; 35R11; 65M12; 65D12.

1. Introduction

Nowadays, in order to understand the dynamics of several physical phenomena, the study of fractional order differential equations is of great importance [4, 6–8, 15, 16, 33]. Because discovering the physical behaviour of a phenomenon in mathematical and engineering sciences, we need the structure of models, which is related to their differential equations [10–12, 20, 25, 26, 32, 34]. The viscoelastic damping and anomalous diffusion process study using differential equations of integer order cannot be done accurately; that is why several authors studied differential models of fractional order [13, 14, 19, 27, 28, 35, 37]. The uses of fractional operators in differential equations is related to hereditary characteristics of several types of materials and processes [2, 21, 36, 41]. Fractional operators describe many features better and more appropriately, such as wave propagation and random walk models.

This paper proposes an efficient numerical approach to obtain an approximate solution to the following diffusion-wave model involving a weakly singular kernel term in the time direction and an integral term in the space direction:

$$\mathcal{D}_t^{\gamma} w(x,y,t) = \frac{1}{\Gamma(\alpha-1)} \int_0^t (t-\lambda)^{\alpha-2} \exp\big(-\upsilon(t-\lambda)\big)\Big(\mathbf{A}_x \frac{\partial^{\vartheta} w(x,y,\lambda)}{\partial |x|^{\vartheta}} + \mathbf{A}_y \frac{\partial^{\nu} w(x,y,\lambda)}{\partial |y|^{\nu}}\Big) d\lambda$$
$$+ \int_0^t \frac{1}{\sqrt{t-\tau}} \Big(\frac{\partial^2 w(x,y,\tau)}{\partial x^2} + \frac{\partial^2 w(x,y,\tau)}{\partial y^2}\Big) d\tau + h(x,y,t), \tag{1.1}$$

Received: 24 February 2025 ; Accepted: 10 August 2025.
∗ Corresponding author. Email: ordokhani@alzahra.ac.ir.

where $\gamma \in (0,1)$, $\vartheta \in (1,2]$, $\nu \in (1,2]$, $\upsilon > 0$ and $\alpha \in (1,2]$ with initial and boundary conditions

$$w(x,y,0) = w_0(x,y),\ (x,y) \in \Omega = [a,b] \times [c,d],$$
$$w(x,y,t) = 0,\ (x,y) \in \partial\Omega,\ t \in (0,T), \tag{1.2}$$

in which the operator $\mathcal{D}_t^{\gamma} w(x,y,t)$ in the time direction shows the Riemann-Liouville fractional derivative and the operators $\frac{\partial^{\vartheta} w(x,y,t)}{\partial |x|^{\vartheta}}$, $\frac{\partial^{\nu} w(x,y,t)}{\partial |y|^{\nu}}$ demonstrate the Riesz fractional opertaors in the space direction which are defined by the formulas

$$\mathcal{D}_t^{\gamma} w(x,y,t) = \frac{1}{\Gamma(1-\gamma)} \frac{\partial}{\partial t} \Big(\int_0^t (t-s)^{-\gamma} w(x,y,s) ds \Big), \tag{1.3}$$

and

$$\frac{\partial^{\vartheta} w(x,y,t)}{\partial |x|^{\vartheta}} = -\Big(2\cos\big(\frac{\pi\vartheta}{2}\big) \Big)^{-1} \Big({}_a\mathbf{D}_x^{\vartheta} w(x,y,t) + {}_x\mathbf{D}_b^{\vartheta} w(x,y,t) \Big), \tag{1.4}$$

$$\frac{\partial^{\nu} w(x,y,t)}{\partial |y|^{\nu}} = -\Big(2\cos\big(\frac{\pi\nu}{2}\big) \Big)^{-1} \Big({}_c\mathbf{D}_y^{\nu} w(x,y,t) + {}_y\mathbf{D}_d^{\nu} w(x,y,t) \Big). \tag{1.5}$$

Also, we define the given fractional operators in Eqs. (1.4) and (1.5) as follows:

$$\begin{aligned}
{}_a\mathbf{D}_x^{\vartheta} w(x,y,t) &= \frac{1}{\Gamma(2-\vartheta)} \frac{\partial^2}{\partial x^2} \Big(\int_a^x (x-s)^{1-\vartheta} w(s,y,t) ds \Big), \\
{}_x\mathbf{D}_b^{\vartheta} w(x,y,t) &= \frac{1}{\Gamma(2-\vartheta)} \frac{\partial^2}{\partial x^2} \Big(\int_x^b (s-x)^{1-\vartheta} w(s,y,t) ds \Big), \\
{}_c\mathbf{D}_y^{\nu} w(x,y,t) &= \frac{1}{\Gamma(2-\nu)} \frac{\partial^2}{\partial y^2} \Big(\int_c^y (y-s)^{1-\nu} w(x,s,t) ds \Big), \\
{}_y\mathbf{D}_d^{\nu} w(x,y,t) &= \frac{1}{\Gamma(2-\nu)} \frac{\partial^2}{\partial y^2} \Big(\int_y^d (s-y)^{1-\nu} w(x,s,t) ds \Big).
\end{aligned} \tag{1.6}$$

The motivation and interest behind considering the above diffusion-wave model with a weakly singular kernel term is that this model is used to describe phenomena where diffusion and wave-like behaviours coexist, influenced by memory effects or hereditary properties. This model often arises in various fields such as heat conduction, fluid flow in porous media, viscoelastic materials, and anomalous transport processes. This model provides a powerful tool for studying complex systems where standard diffusion or wave equations fail to capture the observed phenomena. It bridges the gap between purely diffusive and purely wave-like behaviours, offering insights into processes with memory and anomalous characteristics. The diffusion-wave model with a weakly singular kernel term is important because it provides a robust mathematical framework for describing systems in which both diffusion and wave behaviours are observed, particularly in systems exhibiting memory, nonlocality, and anomalous transport. Its ability to model more complex and realistic behaviours makes it invaluable across a wide range of scientific and engineering disciplines, leading to better predictions, designs, and understanding of real-world phenomena.

To approximate the proposed model presented in Eq. (1.1), a combined numerical approach based on the second-order accurate difference numerical method, the weighted shifted Grünwald derivative approximation, and the Galerkin spectral method is proposed in this study. The second-order accurate difference numerical method and the weighted shifted Grünwald derivative approximation are applied to estimate the integral term, including the Riesz fractional operator and the Riemann–Liouville's fractional operator, respectively. The Galerkin spectral method based on the modified Jacobi functions is applied to approximate the proposed model in the space direction. A convergence study and stability analysis for the presented numerical approach are presented. The reason for using this type of model goes back to studying the effects of the anomalous diffusion process in MRI. In this study, the spatial domain is chosen as $(0,1)$ primarily to simplify the mathematical analysis and numerical implementation. This standard domain enables clearer presentation of the theoretical results, such as stability and error estimates. However, it is important to

emphasize that these results are not inherently restricted to this domain size. When considering an arbitrary domain $(0, L)$ with $L > 1$, the constants involved in the error bounds and stability conditions may depend explicitly on L. This dependence arises because the fractional derivatives, especially those involving non-local operators like the Riesz derivative, inherently reflect the domain size in their integral definitions and boundary behavior.

Obtaining exact solutions of fractional models using analytical methods is not easy; therefore, using numerical approaches to obtain approximate solutions of these types of models has made the work easier. Several authors have proposed different numerical approaches to solve such types of fractional models. For example, in [6], the authors studied a numerical approach based on the finite difference method to obtain approximate solutions of the Bloch-Torrey model of fractional order. In [1], the authors studied the new spectral method for solving the nonlinear differential model of fractional order. In [24], the authors presented the Crank–Nicolson numerical method to calculate the approximate solution of the model along with convergence analysis. The authors in [46] displayed the finite element scheme for obtaining the approximate solutions of the Boussinesq models of fractional order. In [47], the authors proposed a numerical method to obtain approximate solutions of the cable model of fractional order using the finite difference and Legendre spectral numerical method. In [5], the authors proposed the numerical method to obtain approximate solutions of the generalised Schrödinger model involving the Riesz sense using a collocation method. In [45], the authors studied the time-space fractional Bloch-Torrey model and obtained the numerical solutions by applying the $L-2-1_\sigma$ method. In [17], the authors studied the numerical approach based on the Crank-Nicolson extrapolated fully discrete method to obtain the approximate solutions of the fractional model and also examined the convergence analysis for the proposed numerical approach. In [13], the authors proposed the B-spline interpolation and Galerkin finite element method for the two-dimensional Riesz space distributed-order diffusion-wave equation. In [30], the authors studied the finite volume method for solving the fractional model involving the Riesz operator in the space directions. In [31], the authors studied the sinc-Bernoulli collocation method for solving the time fractional cable equation. In [22], the authors presented a numerical approach based on the iterative method to solve the Volterra partial integro–differential models. In [23], the authors presented a numerical approach based on the central difference method and the $L2-1$ method to solve the partial integro–differential model involving the weakly singular kernel. In [44], the authors studied the second-order backward difference method to solve the integro–differential model. In [18], the authors presented a numerical approach based on the stable least residue method to solve the partial integro–differential model involving the weakly singular kernel. In [48], the authors presented a numerical approach based on the Crank–Nicolson ADI spectral method for obtaining the estimated solutions of the two-dimensional nonlinear reaction-diffusion model involving the Riesz space fractional operator. In [39], the authors developed numerical methods suitable for approximating ψ- fractional differential equations and ψ- fractional integro-differential equations. In [40], the Sinc-Galerkin method is recognized for its exponential error decay and, under certain conditions, achieves an optimal convergence rate, even when applied to problems defined on infinite and semi-infinite intervals. In [29], the focus is on the investigation of a (2+1)-dimensional space-time fractional coupled nonlinear Schr ödinger equations, which model the amplitudes of circularly polarized waves in nonlinear optical fibers.

We organise the further manuscript as follows. In section 2, we state the discretisation of the proposed model in terms of the time variable. In this section, the numerical approaches based on the second-order accurate difference numerical method and the weighted shifted Grünwald derivative approximation are studied. As well as this, in this section, the convergence analysis for the semi-discrete numerical approach is studied. In section 3, we present the study of the fully-discrete numerical approach, which states that this numerical approach is based on the Galerkin spectral method. In section 4, we focus on the numerical examples. At the end of this manuscript, the conclusion is displayed in section 5.

2. Discretisation of the proposed model in terms of the time variable

This part studies the numerical approach to approximate the proposed model in the time variable direction. Also, in this section, we state some important lemmas to prove stability and convergence analysis. Assume that $t_n = n\Delta t$, $n = 0, 1, \ldots, \mathcal{N}_t$, and $\Delta t = \frac{T}{\mathcal{N}_t}$. Also, we define the fractional Sobolev space over the Ω domain by

$$\mathcal{H}^{2\beta}(\Omega) = \left\{ w \in L^2(\Omega) \text{ s.t. } (1+\mu^2)^{\frac{1}{2}+\beta} \widetilde{\mathcal{F}}(w)(\mu) \in L^2(\Omega) \right\}, \ \beta \in (0,1), \tag{2.1}$$

in which the symbol $\widetilde{\mathcal{F}}(w)(\mu) = \widetilde{w}$ is the Fourier transformation for the function w and

$$\mathcal{H}_0^{2\beta}(\Omega) = \Big\{ w \in \mathcal{H}^{2\beta}(\Omega) \text{ s.t. } w\Big|_{\partial\Omega} = 0 \Big\}. \tag{2.2}$$

Lemma 2.1. *[3, 42] Assume that $\gamma \in (0,1)$. Then, the numerical approximation based on the shifted Grünwald difference method for the Riemann-Liouville fractional operator in the time direction is obtained as below:*

$$\mathcal{D}_t^{\gamma} w(x,y,t) = \big(\Delta t\big)^{-\gamma} \sum_{l=0}^{n} \sigma_{\gamma}(l) w(x,y,t_{n-l}) + \mathcal{O}\big(\big(\Delta t\big)^2\big), \tag{2.3}$$

in which the parameters given in the above equation are computed by the following formulas:

$$\sigma_{\gamma}(l) = \begin{cases} \frac{\gamma+2}{2}\iota_0^{\gamma}, & l = 0, \\ \frac{\gamma+2}{2}\iota_l^{\gamma} - \frac{\gamma}{2}\iota_{l-1}^{\gamma}, & l > 0, \end{cases} \tag{2.4}$$

where

$$\iota_0^{\gamma} = 1,\ \iota_l^{\gamma} = \frac{\Gamma(l-\gamma)}{\Gamma(-\gamma)\Gamma(l+1)},\ \iota_l^{\gamma} = \frac{l-\gamma-1}{l}\iota_{l-1}^{\gamma},\ l = 1,2,\ldots. \tag{2.5}$$

Also, for real value vector $\Big\{w^n\Big\}_{n=0}^{N\in\mathbb{N}}$, we have the following relations:

$$\begin{aligned} &\sum_{i=0}^{N}\sum_{j=0}^{i} \sigma_{\gamma}(j)\Big\langle w^{i-j}, w^i \Big\rangle \geq 0, \\ &\sum_{j=0}^{i} \sigma_{\gamma}(j) < 0. \end{aligned} \tag{2.6}$$

Lemma 2.2. *[9] Let $1 < \alpha \leq 2$ and $\upsilon \geq 0$. Then, the numerical discretization for fractional integral term in the time direction is obtained as*

$$\frac{1}{\Gamma(\alpha-1)} \int_0^t \big(t-\lambda\big)^{\alpha-2} \exp\big(-\upsilon(t-\lambda)\big) w(x,y,\lambda) d\lambda = \big(\Delta t\big)^{\alpha-1} \sum_{i=0}^{n} \varsigma_i^{\alpha-1} w(x,y,t_{n-i}) + \mathcal{O}\big(\big(\Delta t\big)^2\big), \tag{2.7}$$

in which the values $\varsigma_i^{\alpha-1}$ are given by

$$\varsigma_i^{\alpha-1} = \exp\big(-\upsilon i\Delta t\big)\big(\frac{3}{2}\big)^{1-\alpha} \sum_{j=0}^{i} 3^{-j} f_j^{1-\alpha} f_{i-j}^{1-\alpha}. \tag{2.8}$$

Lemma 2.3. *[43] Suppose that $g(t) \in C^1\big([0,T]\big) \cap \big((0,T)\big)$ and*

$$\mathcal{I}\big(g,t_n\big) = \int_0^t \frac{1}{\sqrt{t_n - \tau}} g(\tau) d\tau. \tag{2.9}$$

Then, the numerical approximation for the given integral term in Eq. (2.9) is calculated as follows:

$$\mathcal{I}\big(g,t_n\big) = c_n g(t_0) + \sum_{p=0}^{n} d_p g(t_{n-p}) + \mathcal{O}\big(\big(\Delta t\big)^{\frac{3}{2}}\big), \tag{2.10}$$

where the coefficients c_n *and* d_n *for* $n = 1, 2, \dots$ *are given by*

$$\begin{aligned}
c_n &= 2\Big(\sqrt{t_n} - (\Delta t)^{-1}\int_{t_n}^{t_{n+1}} \sqrt{\tau}d\tau\Big),\\
d_0 &= 2(\Delta t)^{-1}\int_0^{t_1} \sqrt{\tau}d\tau + \frac{4}{3}\sqrt{\Delta t}\eta,\\
d_1 &= 2(\Delta t)^{-1}\Big(\int_{t_1}^{t_2} \sqrt{\tau}d\tau - \int_{t_0}^{t_1} \sqrt{\tau}d\tau\Big) - \frac{4}{3}\sqrt{\Delta t}\,\eta,\\
d_p &= 2(\Delta t)^{-1}\Big(\int_{t_p}^{t_{p+1}} \sqrt{\tau}d\tau - \int_{t_{p-1}}^{t_p} \sqrt{\tau}d\tau\Big),\ p \geq 2,
\end{aligned} \tag{2.11}$$

in which the constant η *is a nonnegative constant.*

Now we obtain a semi-discrete numerical approach for the presented model (1.1) in the time-variable direction. Then, using Lemmas 2.1, 2.2, and 2.3, we have

$$\begin{aligned}
(\Delta t)^{-\gamma}\sum_{l=0}^{n}\sigma_\gamma(l)w(x,y,t_{n-l}) = (\Delta t)^{\alpha-1}\sum_{i=0}^{n}\varsigma_i^{\alpha-1}\Big(\mathbf{A}_x\frac{\partial^\vartheta w(x,y,t_{n-i})}{\partial|x|^\vartheta} + \mathbf{A}_y\frac{\partial^\nu w(x,y,t_{n-i})}{\partial|y|^\nu}\Big)\\
+ c_n\big(w_{xx}(x,y,0) + w_{yy}(x,y,0)\big)\\
+ \sum_{p=0}^{n} d_p\big(w_{xx}(x,y,t_{n-p}) + w_{yy}(x,y,t_{n-p})\big) + \mathcal{O}\big((\Delta t)^{\frac{3}{2}}\big) + \mathcal{O}\big((\Delta t)^2\big)\\
+ h(x,y,t_n),
\end{aligned} \tag{2.12}$$

in which $\frac{\partial^2 w(x,y,0)}{\partial x^2} = w_{xx}(x,y,0)$ and $\frac{\partial^2 w(x,y,0)}{\partial y^2} = w_{yy}(x,y,0)$. By removing the terms $\mathcal{O}\big((\Delta t)^{\frac{3}{2}}\big)$ and $\mathcal{O}\big((\Delta t)^2\big)$ in the above relation and considering the initial condition $w(x,y,0) = w_0(x,y)$, Eq. (2.12) becomes

$$\begin{aligned}
(\Delta t)^{-\gamma}\sum_{l=0}^{n}\sigma_\gamma(l)W^{n-l} = -(\Delta t)^{\alpha-1}\sum_{i=0}^{n}\varsigma_i^{\alpha-1}\Big(\mathbf{A}_x\frac{\partial^\vartheta W^{n-i}}{\partial|x|^\vartheta} + \mathbf{A}_y\frac{\partial^\nu W^{n-i}}{\partial|y|^\nu}\Big) + c_n\big(\frac{\partial^2 w_0}{\partial x^2} + \frac{\partial^2 w_0}{\partial y^2}\big)\\
+ \sum_{p=0}^{n} d_p\big(\frac{\partial^2 W^{n-p}}{\partial x^2} + \frac{\partial^2 W^{n-p}}{\partial y^2}\big) + h^n,
\end{aligned} \tag{2.13}$$

in which $W(x,y,t_n) = W^n$, $h(x,y,t_n) = h^n$ and W^n is a approximate solution for w. Therefore, the variational weak form of the above equation for each $\varrho \in \mathcal{H}^{\frac{\vartheta}{2}}(\Omega) \cap \mathcal{H}^{\frac{\nu}{2}}(\Omega)$ is written as follows:

$$\begin{aligned}
(\Delta t)^{-\gamma}\sum_{l=0}^{n}\sigma_\gamma(l)\Big\langle W^{n-l}, \varrho\Big\rangle = -(\Delta t)^{\alpha-1}\sum_{i=0}^{n}\varsigma_i^{\alpha-1}\Big(\mathbf{A}_x\Big\langle\frac{\partial^\vartheta W^{n-i}}{\partial|x|^\vartheta}, \varrho\Big\rangle + \mathbf{A}_y\Big\langle\frac{\partial^\nu W^{n-i}}{\partial|y|^\nu}, \varrho\Big\rangle\Big) + c_n\Big\langle\Delta w_0, \varrho\Big\rangle\\
+ \sum_{p=0}^{n} d_p\Big(\Big\langle\frac{\partial^2 W^{n-p}}{\partial x^2}, \varrho\Big\rangle + \Big\langle\frac{\partial^2 W^{n-p}}{\partial y^2}, \varrho\Big\rangle\Big) + \Big\langle h^n, \varrho\Big\rangle,
\end{aligned} \tag{2.14}$$

in which $\Delta w_0 = \big(\frac{\partial^2 w_0}{\partial x^2} + \frac{\partial^2 w_0}{\partial y^2}\big)$. Therefore, we can rewrite the Equation (2.14) as follows:

$$\begin{aligned}
(\Delta t)^{-\gamma}\sum_{l=0}^{n}\sigma_\gamma(l)\Big\langle W^{n-l}, \varrho\Big\rangle = -(\Delta t)^{\alpha-1}\sum_{i=0}^{n}\varsigma_i^{\alpha-1}\mathcal{B}\Big\langle W^{n-i}, \varrho\Big\rangle + c_n\Big\langle\Delta w_0, \varrho\Big\rangle\\
- \sum_{p=0}^{n} d_p\Big\langle\nabla W^{n-p}, \nabla\varrho\Big\rangle + \Big\langle h^n, \varrho\Big\rangle,
\end{aligned} \tag{2.15}$$

where

$$\mathcal{B}\Big\langle W^n,\varrho\Big\rangle=\mathbf{A}_x\kappa_1\Big\{\Big\langle {}_a\mathbf{D}_x^{\frac{\vartheta}{2}}W^n,{}_x\mathbf{D}_b^{\frac{\vartheta}{2}}\varrho\Big\rangle+\Big\langle {}_x\mathbf{D}_b^{\frac{\vartheta}{2}}W^n,{}_a\mathbf{D}_x^{\frac{\vartheta}{2}}\varrho\Big\rangle\Big\}$$
$$+\mathbf{A}_y\kappa_2\Big\{\Big\langle {}_c\mathbf{D}_y^{\frac{\nu}{2}}W^n,{}_y\mathbf{D}_d^{\frac{\nu}{2}}\varrho\Big\rangle+\Big\langle {}_y\mathbf{D}_d^{\frac{\nu}{2}}W^n,{}_c\mathbf{D}_y^{\frac{\nu}{2}}\varrho\Big\rangle\Big\},\tag{2.16}$$

and $\kappa_1=\Big(2\cos\big(\frac{\pi\vartheta}{2}\big)\Big)^{-1}$, $\kappa_2=\Big(2\cos\big(\frac{\pi\nu}{2}\big)\Big)^{-1}$.

Lemma 2.4. *[38] Assume that the sequences x_n and y_n be two sequences such that the following inequality is true:*

$$\begin{cases} y_0\le\delta_0,\\ y_0\le\delta_0+\sum_{i=0}^{n-1}\varpi_i+\sum_{i=0}^{n-1}x_iy_i,\quad n\ge 1,\end{cases}\tag{2.17}$$

in which x_n is a nonnegative sequence. Then, if $\delta_0\ge 0$ and $\varpi_0\ge 0$, we have

$$y_n\le\Big\{\delta_0+\sum_{i=0}^{n-1}\varpi_i\Big\}\exp\Big(\sum_{i=0}^{n-1}x_i\Big),\ n=1,2,\ldots.\tag{2.18}$$

Theorem 2.5. *Suppose that $W^n\in\mathcal{H}^{\frac{\vartheta}{2}}(\Omega)\cap\mathcal{H}^{\frac{\nu}{2}}(\Omega)$. Then, the semi-discrete numerical approximation obtained in Eq. (2.15) is unconditionally stable.*

Proof. To prove this theorem, we introduce the symbol $\mathcal{E}^n=W^n-\widetilde{W}^n$ that $\mathcal{E}^n$ shows the roundoff error term and $\widetilde{W}^n$ is the approximate solution for Eq. (2.15). Thus, for each $\varrho\in\in\mathcal{H}^{\frac{\vartheta}{2}}(\Omega)\cap\mathcal{H}^{\frac{\nu}{2}}(\Omega)$, we obtain the following equation:

$$(\Delta t)^{-\gamma}\sum_{l=0}^{n}\sigma_\gamma(l)\Big\langle\mathcal{E}^{n-l},\varrho\Big\rangle=-(\Delta t)^{\alpha-1}\sum_{i=0}^{n}\varsigma_i^{\alpha-1}\mathcal{B}\Big\langle\mathcal{E}^{n-i},\varrho\Big\rangle+c_n\Big\langle\Delta\mathcal{E}^0,\varrho\Big\rangle-\sum_{p=0}^{n}d_p\Big\langle\nabla\mathcal{E}^{n-p},\nabla\varrho\Big\rangle.\tag{2.19}$$

By inserting the value $\varrho=\mathcal{E}^n$ into the above equation, we get

$$(\Delta t)^{-\gamma}\sum_{l=0}^{n}\sigma_\gamma(l)\Big\langle\mathcal{E}^{n-l},\mathcal{E}^n\Big\rangle=-(\Delta t)^{\alpha-1}\sum_{i=0}^{n}\varsigma_i^{\alpha-1}\mathcal{B}\Big\langle\mathcal{E}^{n-i},\mathcal{E}^n\Big\rangle+c_n\Big\langle\Delta\mathcal{E}^0,\mathcal{E}^n\Big\rangle-\sum_{p=0}^{n}d_p\Big\langle\nabla\mathcal{E}^{n-p},\nabla\mathcal{E}^n\Big\rangle.\tag{2.20}$$

Also, we have

$$\begin{aligned}\Big|\mathcal{B}\Big\langle\mathcal{E}^n,\mathcal{E}^n\Big\rangle\Big|&\le\Big|\mathbf{A}_x\kappa_1\Big|\Big\{\Big|\Big\langle {}_a\mathbf{D}_x^{\frac{\vartheta}{2}}\mathcal{E}^n,{}_x\mathbf{D}_b^{\frac{\vartheta}{2}}\mathcal{E}^n\Big\rangle\Big|+\Big|\Big\langle {}_x\mathbf{D}_b^{\frac{\vartheta}{2}}\mathcal{E}^n,{}_a\mathbf{D}_x^{\frac{\vartheta}{2}}\mathcal{E}^n\Big\rangle\Big|\Big\}\\&+\Big|\mathbf{A}_y\kappa_2\Big|\Big\{\Big|\Big\langle {}_c\mathbf{D}_y^{\frac{\nu}{2}}\mathcal{E}^n,{}_y\mathbf{D}_d^{\frac{\nu}{2}}\mathcal{E}^n\Big\rangle\Big|+\Big|\Big\langle {}_y\mathbf{D}_d^{\frac{\nu}{2}}\mathcal{E}^n,{}_c\mathbf{D}_y^{\frac{\nu}{2}}\mathcal{E}^n\Big\rangle\Big|\Big\}\\&\le\Big|\mathbf{A}_x\kappa_1\Big|\Big\{\parallel {}_a\mathbf{D}_x^{\frac{\vartheta}{2}}\mathcal{E}^n\parallel_0\parallel {}_x\mathbf{D}_b^{\frac{\vartheta}{2}}\mathcal{E}^n\parallel_0+\parallel {}_x\mathbf{D}_b^{\frac{\vartheta}{2}}\mathcal{E}^n\parallel_0\parallel {}_a\mathbf{D}_x^{\frac{\vartheta}{2}}\mathcal{E}^n\parallel_0\Big\}\\&+\Big|\mathbf{A}_y\kappa_2\Big|\Big\{\parallel {}_c\mathbf{D}_y^{\frac{\nu}{2}}\mathcal{E}^n\parallel_0\parallel {}_y\mathbf{D}_d^{\frac{\nu}{2}}\mathcal{E}^n\parallel_0+\parallel {}_y\mathbf{D}_d^{\frac{\nu}{2}}\mathcal{E}^n\parallel_0\parallel {}_c\mathbf{D}_y^{\frac{\nu}{2}}\mathcal{E}^n\parallel_0\Big\}\\&\le\mathcal{C}_3\parallel\mathcal{E}^n\parallel^2_{\mathcal{H}^{\frac{\vartheta}{2}}(\Omega)\cap\mathcal{H}^{\frac{\nu}{2}}(\Omega)},\end{aligned}\tag{2.21}$$

in which $\mathcal{C}_3=\Big|\mathcal{C}_1\mathcal{A}_x\kappa_1\Big|+\Big|\mathcal{C}_2\mathcal{A}_y\kappa_2\Big|$. As well as,

$$\begin{aligned}\Big|\mathcal{B}\Big\langle\mathcal{E}^n,\mathcal{E}^n\Big\rangle\Big|&\ge|2\mathcal{A}_x\kappa_1|\Big|\Big\langle {}_a\mathbf{D}_x^{\frac{\vartheta}{2}}\mathcal{E}^n,{}_x\mathbf{D}_b^{\frac{\vartheta}{2}}\mathcal{E}^n\Big\rangle\Big|+|2\mathcal{A}_y\kappa_2|\Big|\Big\langle {}_c\mathbf{D}_y^{\frac{\nu}{2}}\mathcal{E}^n,{}_y\mathbf{D}_d^{\frac{\nu}{2}}\mathcal{E}^n\Big\rangle\Big|\\&\ge\min\big(|2\mathcal{A}_x\kappa_1|,|2\mathcal{A}_y\kappa_2|\big)\Big\{\Big|\Big\langle {}_a\mathbf{D}_x^{\frac{\vartheta}{2}}\mathcal{E}^n,{}_x\mathbf{D}_b^{\frac{\vartheta}{2}}\mathcal{E}^n\Big\rangle\Big|+\Big|\Big\langle {}_c\mathbf{D}_y^{\frac{\nu}{2}}\mathcal{E}^n,{}_y\mathbf{D}_d^{\frac{\nu}{2}}\mathcal{E}^n\Big\rangle\Big|\Big\}\\&\ge\mathcal{C}_5\parallel\mathcal{E}^n\parallel^2_{\mathcal{H}^{\frac{\vartheta}{2}}(\Omega)\cap\mathcal{H}^{\frac{\nu}{2}}(\Omega)},\end{aligned}\tag{2.22}$$

in which $\mathcal{C}_5=\mathcal{C}_4\min\big(|2\mathcal{A}_x\kappa_1|,|2\mathcal{A}_y\kappa_2|\big)$. With summation on the index n from 0 to $\mathcal{N}$ for Eq. (2.20), we get

$$(\Delta t)^{-\gamma}\sum_{n=0}^{\mathcal{N}}\sum_{l=0}^{n}\sigma_\gamma(l)\Big\langle\mathcal{E}^{n-l},\mathcal{E}^n\Big\rangle=-(\Delta t)^{\alpha-1}\sum_{n=0}^{\mathcal{N}}\sum_{i=0}^{n}\varsigma_i^{\alpha-1}\mathcal{B}\Big\langle\mathcal{E}^{n-i},\mathcal{E}^n\Big\rangle+\sum_{n=0}^{\mathcal{N}}c_n\Big\langle\Delta\mathcal{E}^0,\mathcal{E}^n\Big\rangle-\sum_{n=0}^{\mathcal{N}}\sum_{p=0}^{n}d_p\Big\langle\nabla\mathcal{E}^{n-p},\nabla\mathcal{E}^n\Big\rangle.\tag{2.23}$$

Applying Lemma 2.1, we have

$$(\Delta t)^{\alpha-1}\sum_{n=0}^{\mathcal{N}}\sum_{i=0}^{n}\varsigma_i^{\alpha-1}\mathcal{B}\Big\langle\mathcal{E}^{n-i},\mathcal{E}^{n}\Big\rangle\geq 0, \tag{2.24}$$

and

$$-\sum_{n=0}^{\mathcal{N}}\sum_{p=0}^{n}d_p\Big\langle\nabla\mathcal{E}^{n-p},\nabla\mathcal{E}^{n}\Big\rangle\leq 0. \tag{2.25}$$

As well as, from Eq. (2.22), we get

$$(\Delta t)^{\alpha-1}\sum_{n=0}^{\mathcal{N}}\sum_{i=0}^{n}\varsigma_i^{\alpha-1}\mathcal{B}\Big\langle\mathcal{E}^{n-i},\mathcal{E}^{n}\Big\rangle\geq(\Delta t)^{\alpha-1}\sum_{n=0}^{\mathcal{N}}\sum_{i=0}^{n}\varsigma_i^{\alpha-1}\mathcal{C}_5\parallel\mathcal{E}^{n}\parallel^2_{\mathcal{H}^{\frac{\vartheta}{2}}(\Omega)\cap\mathcal{H}^{\frac{\nu}{2}}(\Omega)}. \tag{2.26}$$

Thus, using Eqs. (2.25) and (2.26), we have

$$(\Delta t)^{-\gamma}\sum_{n=0}^{\mathcal{N}}\sum_{l=0}^{n}\sigma_\gamma(l)\parallel\mathcal{E}^{n}\parallel^2_{\mathcal{H}^{\frac{\vartheta}{2}}(\Omega)\cap\mathcal{H}^{\frac{\nu}{2}}(\Omega)}\leq\sum_{n=0}^{\mathcal{N}}c_n\Big\langle\Delta\mathcal{E}^{0},\mathcal{E}^{n}\Big\rangle. \tag{2.27}$$

By changing the index, we obtain

$$(\Delta t)^{-\gamma}\sum_{i=0}^{n}\sum_{l=0}^{i}\sigma_\gamma(l)\parallel\mathcal{E}^{i}\parallel^2_{\mathcal{H}^{\frac{\vartheta}{2}}(\Omega)\cap\mathcal{H}^{\frac{\nu}{2}}(\Omega)}\leq\sum_{i=0}^{n}c_i\Big\langle\Delta\mathcal{E}^{0},\mathcal{E}^{i}\Big\rangle. \tag{2.28}$$

Therefore,

$$\begin{aligned}\parallel\mathcal{E}^{n}\parallel^2_{L^2(\Omega)}&\leq(\Delta t)^{-\gamma}\sum_{i=0}^{n}\sum_{l=0}^{i}\sigma_\gamma(l)\parallel\mathcal{E}^{i}\parallel^2_{\mathcal{H}^{\frac{\vartheta}{2}}(\Omega)\cap\mathcal{H}^{\frac{\nu}{2}}(\Omega)}\leq\sum_{i=0}^{n}c_i\Big\langle\Delta\mathcal{E}^{0},\mathcal{E}^{i}\Big\rangle\\&\leq c_0\Big\langle\Delta\mathcal{E}^{0},\mathcal{E}^{0}\Big\rangle+\sum_{i=1}^{n}c_i\Big\langle\Delta\mathcal{E}^{0},\mathcal{E}^{i}\Big\rangle\\&\leq|c_0|\parallel\nabla\mathcal{E}^{0}\parallel^2_{L^2(\Omega)}+\parallel\Delta\mathcal{E}^{0}\parallel_{L^2(\Omega)}\sum_{i=1}^{n}c_i\parallel\mathcal{E}^{i}\parallel_{L^2(\Omega)}\\&\leq 1+|c_0|\parallel\nabla\mathcal{E}^{0}\parallel^2_{L^2(\Omega)}+\parallel\Delta\mathcal{E}^{0}\parallel_{L^2(\Omega)}\sum_{i=1}^{n}c_i\parallel\mathcal{E}^{i}\parallel_{L^2(\Omega)}.\end{aligned} \tag{2.29}$$

Then, from the above relation, we have

$$\parallel\mathcal{E}^{n}\parallel^2_{L^2(\Omega)}\leq 1+|c_0|\parallel\nabla\mathcal{E}^{0}\parallel^2_{L^2(\Omega)}+\parallel\Delta\mathcal{E}^{0}\parallel_{L^2(\Omega)}\sum_{i=1}^{n}c_i\parallel\mathcal{E}^{i}\parallel_{L^2(\Omega)}. \tag{2.30}$$

Since $\sum_{i=1}^{n}c_i\leq\sum_{i=1}^{n}(c_i)^2$, then

$$\begin{aligned}\parallel\mathcal{E}^{n}\parallel^2_{L^2(\Omega)}&\leq 1+|c_0|\parallel\nabla\mathcal{E}^{0}\parallel^2_{L^2(\Omega)}+\parallel\Delta\mathcal{E}^{0}\parallel_{L^2(\Omega)}\Delta t\sum_{i=1}^{n}\frac{1}{\Delta t}(c_i)^2\parallel\mathcal{E}^{i}\parallel_{L^2(\Omega)}\\&\leq\Big\{1+|c_0|\parallel\nabla\mathcal{E}^{0}\parallel^2_{L^2(\Omega)}\Big\}\exp\Big(\Delta t\parallel\Delta\mathcal{E}^{0}\parallel_{L^2(\Omega)}\sum_{i=1}^{n}\frac{1}{\Delta t}(c_i)^2\Big)\\&\leq\Big\{1+|c_0|\parallel\nabla\mathcal{E}^{0}\parallel^2_{L^2(\Omega)}\Big\}\exp\Big(\mathbb{C}\Big(\sum_{i=1}^{n}c_i\Big)^2\Big)\Big\{1+|c_0|\parallel\nabla\mathcal{E}^{0}\parallel^2_{L^2(\Omega)}\Big\}\exp\Big(\mathbb{C}\Delta t\Big).\end{aligned} \tag{2.31}$$

Therefore, the above inequality shows that the semi-discrete numerical approach for the presented model (1.1), which is displayed in Eq. (2.15), is unconditionally stable. □

Theorem 2.6. *Suppose that* $w^n, W^n \in \mathcal{H}^{\frac{\vartheta}{2}}(\Omega) \cap \mathcal{H}^{\frac{\nu}{2}}(\Omega)$. *Then, the semi-discrete numerical approximation, which is obtained in Eq.* (2.15), *is convergent.*

Proof. Since w^n and W^n are the exact and approximate solution of Eq. (1.1), then from Eqs. (2.12) and (2.13), we have

$$(\Delta t)^{-\gamma}\sum_{l=0}^{n}\sigma_\gamma(l)w^{n-l} = -(\Delta t)^{\alpha-1}\sum_{i=0}^{n}\varsigma_i^{\alpha-1}\Big(\mathbf{A}_x\frac{\partial^\vartheta w^{n-i}}{\partial|x|^\vartheta}+\mathbf{A}_y\frac{\partial^\nu w^{n-i}}{\partial|y|^\nu}\Big)+c_n\big(\frac{\partial^2 w_0}{\partial x^2}+\frac{\partial^2 w_0}{\partial y^2}\big)$$
$$+\sum_{p=0}^{n}d_p\big(\frac{\partial^2 w^{n-p}}{\partial x^2}+\frac{\partial^2 w^{n-p}}{\partial y^2}\big)+h^n+\mathcal{R}_{\Delta t}, \tag{2.32}$$

and

$$(\Delta t)^{-\gamma}\sum_{l=0}^{n}\sigma_\gamma(l)W^{n-l} = -(\Delta t)^{\alpha-1}\sum_{i=0}^{n}\varsigma_i^{\alpha-1}\Big(\mathbf{A}_x\frac{\partial^\vartheta W^{n-i}}{\partial|x|^\vartheta}+\mathbf{A}_y\frac{\partial^\nu W^{n-i}}{\partial|y|^\nu}\Big)+c_n\big(\frac{\partial^2 w_0}{\partial x^2}+\frac{\partial^2 w_0}{\partial y^2}\big)$$
$$+\sum_{p=0}^{n}d_p\big(\frac{\partial^2 W^{n-p}}{\partial x^2}+\frac{\partial^2 W^{n-p}}{\partial y^2}\big)+h^n, \tag{2.33}$$

in which $\left|\mathcal{R}_{\Delta t}\right| \le \mathcal{C}_6(\Delta t)^{\frac{3}{2}}$. Therefore, by subtracting the above two relations from each other and defining the symbol $\mathcal{P}^n = w^n - W^n$, we have

$$(\Delta t)^{-\gamma}\sum_{l=0}^{n}\sigma_\gamma(l)\mathcal{P}^{n-l} = -(\Delta t)^{\alpha-1}\sum_{i=0}^{n}\varsigma_i^{\alpha-1}\Big(\mathbf{A}_x\frac{\partial^\vartheta \mathcal{P}^{n-i}}{\partial|x|^\vartheta}+\mathbf{A}_y\frac{\partial^\nu \mathcal{P}^{n-i}}{\partial|y|^\nu}\Big)$$
$$+\sum_{p=0}^{n}d_p\big(\frac{\partial^2 \mathcal{P}^{n-p}}{\partial x^2}+\frac{\partial^2 \mathcal{P}^{n-p}}{\partial y^2}\big)+\mathcal{R}_{\Delta t}. \tag{2.34}$$

Thus, for each $\varrho \in\in \mathcal{H}^{\frac{\vartheta}{2}}(\Omega) \cap \mathcal{H}^{\frac{\nu}{2}}(\Omega)$, we get the variational weak form of Eq. (2.34) as follows:

$$(\Delta t)^{-\gamma}\sum_{l=0}^{n}\sigma_\gamma(l)\Big\langle\mathcal{P}^{n-l},\varrho\Big\rangle = -(\Delta t)^{\alpha-1}\sum_{i=0}^{n}\varsigma_i^{\alpha-1}\mathcal{B}\Big\langle\mathcal{P}^{n-i},\varrho\Big\rangle-\sum_{p=0}^{n}d_p\Big\langle\nabla\mathcal{P}^{n-p},\nabla\varrho\Big\rangle+\Big\langle\mathcal{R}_{\Delta t},\varrho\Big\rangle. \tag{2.35}$$

To continue proving this theorem, we put $\varrho = \mathcal{P}^n$, then

$$(\Delta t)^{-\gamma}\sum_{l=0}^{n}\sigma_\gamma(l)\Big\langle\mathcal{P}^{n-l},\mathcal{P}^n\Big\rangle = -(\Delta t)^{\alpha-1}\sum_{i=0}^{n}\varsigma_i^{\alpha-1}\mathcal{B}\Big\langle\mathcal{P}^{n-i},\mathcal{P}^n\Big\rangle-\sum_{p=0}^{n}d_p\Big\langle\nabla\mathcal{P}^{n-p},\nabla\mathcal{P}^n\Big\rangle+\Big\langle\mathcal{R}_{\Delta t},\mathcal{P}^n\Big\rangle. \tag{2.36}$$

By summing the above equation on the index n from 0 to $\mathcal{N}$, we get

$$(\Delta t)^{-\gamma}\sum_{n=0}^{\mathcal{N}}\sum_{l=0}^{n}\sigma_\gamma(l)\Big\langle\mathcal{P}^{n-l},\mathcal{P}^n\Big\rangle = -(\Delta t)^{\alpha-1}\sum_{n=0}^{\mathcal{N}}\sum_{i=0}^{n}\varsigma_i^{\alpha-1}\mathcal{B}\Big\langle\mathcal{P}^{n-i},\mathcal{P}^n\Big\rangle$$
$$-\sum_{n=0}^{\mathcal{N}}\sum_{p=0}^{n}d_p\Big\langle\nabla\mathcal{P}^{n-p},\nabla\mathcal{P}^n\Big\rangle+\sum_{n=0}^{\mathcal{N}}\Big\langle\mathcal{R}_{\Delta t},\mathcal{P}^n\Big\rangle. \tag{2.37}$$

By using Lemma 2.1, we have

$$(\Delta t)^{\alpha-1}\sum_{n=0}^{\mathcal{N}}\sum_{i=0}^{n}\varsigma_i^{\alpha-1}\mathcal{B}\Big\langle\mathcal{P}^{n-i},\mathcal{P}^n\Big\rangle \ge 0, \tag{2.38}$$

and

$$-\sum_{n=0}^{\mathcal{N}}\sum_{p=0}^{n}d_p\Big\langle\nabla\mathcal{P}^{n-p},\nabla\mathcal{P}^n\Big\rangle \le 0. \tag{2.39}$$

Moreover, from Eq. (2.22), we conclude that

$$(\Delta t)^{\alpha-1}\sum_{n=0}^{\mathcal{N}}\sum_{i=0}^{n}\varsigma_i^{\alpha-1}\mathcal{B}\Big\langle \mathcal{P}^{n-i},\mathcal{P}^{n}\Big\rangle \geq (\Delta t)^{\alpha-1}\sum_{n=0}^{\mathcal{N}}\sum_{i=0}^{n}\varsigma_i^{\alpha-1}\mathcal{C}_5 \parallel \mathcal{P}^{n} \parallel^2_{\mathcal{H}^{\frac{\vartheta}{2}}(\Omega)\cap\mathcal{H}^{\frac{\nu}{2}}(\Omega)}. \tag{2.40}$$

So, using the relations (2.38), (2.39) and (2.40), we have

$$\begin{aligned}
\parallel \mathcal{P}^{n} \parallel^2_{L^2(\Omega)} &\leq (\Delta t)^{-\gamma}\sum_{i=0}^{n}\sum_{l=0}^{i}\sigma_\gamma(l) \parallel \mathcal{P}^{i} \parallel^2_{\mathcal{H}^{\frac{\vartheta}{2}}(\Omega)\cap\mathcal{H}^{\frac{\nu}{2}}(\Omega)} \leq \sum_{i=0}^{n}\Big\langle \mathcal{R}_{\Delta t},\mathcal{P}^{n}\Big\rangle \\
&\leq \sum_{i=0}^{n} \parallel \mathcal{P}^{n} \parallel_{L^2(\Omega)} \parallel \mathcal{R}_{\Delta t} \parallel_{L^2(\Omega)} = \mathcal{C}_6(\Delta t)^{\frac{3}{2}}\sum_{i=0}^{n} \parallel \mathcal{P}^{n} \parallel_{L^2(\Omega)} = \mathcal{C}_6\Delta t\sum_{i=0}^{n}\sqrt{\Delta t} \parallel \mathcal{P}^{n} \parallel_{L^2(\Omega)} \\
&\leq \frac{1}{2}\mathcal{C}_6\Delta t\Big\{\sum_{i=0}^{n}\Delta t+\sum_{i=0}^{n} \parallel \mathcal{P}^{n} \parallel^2_{L^2(\Omega)}\Big\} \leq \frac{1}{2}\mathcal{C}_6\Delta t\Big\{T+\sum_{i=0}^{n} \parallel \mathcal{P}^{n} \parallel^2_{L^2(\Omega)}\Big\} \\
&\leq \mathcal{C}_6\Delta tT+\mathcal{C}_6\Delta t\sum_{i=0}^{n} \parallel \mathcal{P}^{n} \parallel^2_{L^2(\Omega)}.
\end{aligned} \tag{2.41}$$

Thus

$$\parallel \mathcal{P}^{n} \parallel^2_{L^2(\Omega)} \leq \mathcal{C}_6\Delta tT+\mathcal{C}_6\Delta t\sum_{i=0}^{n} \parallel \mathcal{P}^{n} \parallel^2_{L^2(\Omega)} \leq \mathcal{C}_6\Delta tT\exp\Big(\mathcal{C}_6T\Delta t(n+1)\Big) \leq \mathcal{C}_*\Delta t. \tag{2.42}$$

The above equation show that the semi-discrete numerical approximation which is obtained in Eq. (2.15), is convergent. □

3. Fully-discrete numerical approach

This section focuses on the approximation of the presented model based on the general Jacobi functions [36] in terms of the space variables. Here we define the weighted Sobolev space on the domain Ω by the following set

$$L^2_\omega(\Omega)=\Big\{w:\ \int_\Omega w^2(x)\omega(x)\,dx<+\infty\Big\}, \tag{3.1}$$

in which the symbol $\omega(x)$ shows the weight function and the defined norm for this the weighted Sobolev space defined by

$$\parallel w \parallel^2_{L^2_\omega(\Omega)}=\int_\Omega w^2(x)\omega(x)\,dx. \tag{3.2}$$

Also, we consider the following set with the given values $\rho\in(1,2)$, $\zeta\in(0,\rho)$, $\zeta\in(0,\rho)$, $\theta=-1,0,1,\ldots,m$ such that $m\in\mathbb{N}$:

$$\mathcal{V}^m_{\rho,p,\xi,\zeta}=\Big\{w\in L^2_{\omega^{-\xi,-\zeta}}(\Omega):\ \ \mathcal{D}_p^{\rho+1}w\in L^2_{\omega^{\zeta+\theta,\xi+\theta}}(\Omega)\Big\}, \tag{3.3}$$

where the symbol $\mathcal{D}_p^{\rho+1}w$ shows the two-sided fractional operators. Here the space $\mathcal{V}^m_{\rho,p,\xi,\zeta}$ demonstrates the non-uniform Jacobi weighted space. We introduce the polynomial space of fractional order with finite dimensional as

$$\mathcal{Q}^{-\xi,-\zeta}_{\mathcal{N}}(\Omega)=\Big\{\psi=(1-x)^{\xi}(1+x)^{\zeta}\varphi:\ \ \varphi\in\mathcal{K}_{\mathcal{N}}\Big\}, \tag{3.4}$$

in which $\mathcal{K}_{\mathcal{N}}$ is the set of polynomials of $\mathcal{N}$ degree. Now we display the projection operator by the following map:

$$\Pi_h:\ \mathcal{H}^{\vartheta}_0(\Omega)\cap\mathcal{H}^{\nu}_0(\Omega)\cap C^0(\Omega)\to X_h, \tag{3.5}$$

where

$$\mathcal{B}\Big\langle\Pi_h z,u\Big\rangle,\ \ \forall u\in X_h, \tag{3.6}$$

and X_h is the finite element space. Also, for each $w \in \mathcal{H}^o(\Omega)$ that $o = 1, 2, \ldots, m$, we have

$$\| w - \mathrm{P}_h^m w \|_{\mathcal{H}^o(\Omega)} \leq \mathcal{C}_{**} h^{m-o} \| w \|_{\mathcal{H}^o(\Omega)}, \tag{3.7}$$

in which P_h^m shows the interpolation operator. Thus, the variational weak form of Eq. (1.1) using the fully discrete numerical approach for each $\Phi_h \in \mathcal{H}_0^{\vartheta}(\Omega) \cap \mathcal{H}_0^{\nu}(\Omega) \cap C^0(\Omega)$ is obtained as follows:

$$\begin{aligned}(\Delta t)^{-\gamma} \sum_{l=0}^{n} \sigma_\gamma(l) \Big\langle W_h^{n-l}, \Phi_h \Big\rangle = -(\Delta t)^{\alpha-1} \sum_{i=0}^{n} \varsigma_i^{\alpha-1} \mathcal{B} \Big\langle W_h^{n-i}, \Phi_h \Big\rangle + c_n \Big\langle \Delta w_0, \Phi_h \Big\rangle \\ - \sum_{p=0}^{n} d_p \Big\langle \nabla W_h^{n-p}, \nabla \Phi_h \Big\rangle + \Big\langle h^n, \Phi_h \Big\rangle.\end{aligned} \tag{3.8}$$

In the above equation, we find $W_h^n \in \mathcal{H}_0^{\vartheta}(\Omega) \cap \mathcal{H}_0^{\nu}(\Omega) \cap C^0(\Omega)$.

Lemma 3.1. *[6] Assume that $w \in \mathcal{H}_0^{\vartheta}(\Omega) \cap \mathcal{H}_0^{\nu}(\Omega)$ and $\nu \leq \vartheta \leq k+1$. Then*

$$\| w - \Pi_h w \|_{\mathcal{H}_0^{\nu}(\Omega)} \leq \mathcal{C} h^{\vartheta-\nu} \| w \|_{\mathcal{H}_0^{\vartheta}(\Omega)}. \tag{3.9}$$

Theorem 3.2. *Suppose that $w(x, y, t_n) = w^n \in \mathcal{H}_0^{\vartheta}(\Omega) \cap \mathcal{H}_0^{\nu}(\Omega)$ be the exact solution of Eq. (1.1) and $W_h^n \in X_h$ is the approximate solution for Eq. (1.1). Then, we obtain the following inequality:*

$$\| w^n - W_h^n \|_{\mathcal{H}_0^{\vartheta}(\Omega)} \leq \mathcal{C}_7 \big((\Delta t)^{\frac{3}{2}} + h^{\vartheta-\nu} \big). \tag{3.10}$$

Proof. Since w^n and W^n are the exact and approximate solution of Eq. (1.1), then

$$\begin{aligned}(\Delta t)^{-\gamma} \sum_{l=0}^{n} \sigma_\gamma(l) w^{n-l} = -(\Delta t)^{\alpha-1} \sum_{i=0}^{n} \varsigma_i^{\alpha-1} \Big(\mathbf{A}_x \frac{\partial^{\vartheta} w^{n-i}}{\partial |x|^{\vartheta}} + \mathbf{A}_y \frac{\partial^{\nu} w^{n-i}}{\partial |y|^{\nu}} \Big) + c_n \big(\frac{\partial^2 w_0}{\partial x^2} + \frac{\partial^2 w_0}{\partial y^2} \big) \\ + \sum_{p=0}^{n} d_p \big(\frac{\partial^2 w^{n-p}}{\partial x^2} + \frac{\partial^2 w^{n-p}}{\partial y^2} \big) + h^n + \mathcal{R}_{\Delta t},\end{aligned} \tag{3.11}$$

and

$$\begin{aligned}(\Delta t)^{-\gamma} \sum_{l=0}^{n} \sigma_\gamma(l) W_h^{n-l} = -(\Delta t)^{\alpha-1} \sum_{i=0}^{n} \varsigma_i^{\alpha-1} \Big(\mathbf{A}_x \frac{\partial^{\vartheta} W_h^{n-i}}{\partial |x|^{\vartheta}} + \mathbf{A}_y \frac{\partial^{\nu} W_h^{n-i}}{\partial |y|^{\nu}} \Big) + c_n \big(\frac{\partial^2 w_0}{\partial x^2} + \frac{\partial^2 w_0}{\partial y^2} \big) \\ + \sum_{p=0}^{n} d_p \big(\frac{\partial^2 W_h^{n-p}}{\partial x^2} + \frac{\partial^2 W_h^{n-p}}{\partial y^2} \big) + h^n.\end{aligned} \tag{3.12}$$

By subtracting the above relations from each other, we conclude that:

$$\begin{aligned}(\Delta t)^{-\gamma} \sum_{l=0}^{n} \sigma_\gamma(l) \big(w^{n-l} - W_h^{n-l} \big) = -(\Delta t)^{\alpha-1} \sum_{i=0}^{n} \varsigma_i^{\alpha-1} \Big(\mathbf{A}_x \frac{\partial^{\vartheta} \big(w^{n-i} - W_h^{n-i} \big)}{\partial |x|^{\vartheta}} + \mathbf{A}_y \frac{\partial^{\nu} \big(w^{n-i} - W_h^{n-i} \big)}{\partial |y|^{\nu}} \Big) \\ + \sum_{p=0}^{n} d_p \big(\frac{\partial^2 \big(w^{n-p} - W_h^{n-p} \big)}{\partial x^2} + \frac{\partial^2 \big(w^{n-p} - W_h^{n-p} \big)}{\partial y^2} \big) + \mathcal{R}_{\Delta t}.\end{aligned} \tag{3.13}$$

So, the weak variational form of the above equation for each $\varrho \in \mathcal{H}_0^{\vartheta}(\Omega) \cap \mathcal{H}_0^{\nu}(\Omega)$ is obtained as follows:

$$\begin{aligned}(\Delta t)^{-\gamma} \sum_{l=0}^{n} \sigma_\gamma(l) \Big\langle w^{n-l} - W_h^{n-l}, \varrho \Big\rangle = -(\Delta t)^{\alpha-1} \sum_{i=0}^{n} \varsigma_i^{\alpha-1} \mathcal{B} \Big\langle w^{n-i} - W_h^{n-i}, \varrho \Big\rangle \\ - \sum_{p=0}^{n} d_p \Big\langle \nabla \big(w^{n-p} - W_h^{n-p} \big), \nabla \varrho \Big\rangle + \Big\langle \mathcal{R}_{\Delta t}, \varrho \Big\rangle.\end{aligned} \tag{3.14}$$

For the proof process, we introduce the following symbols:

$$\Psi_h^n = \Pi_h w^n - W_h^n, \quad \Upsilon_h^n = w^n - \Pi_h w^n. \tag{3.15}$$

Thus,

$$\begin{aligned}(\Delta t)^{-\gamma}\sum_{l=0}^{n}\sigma_\gamma(l)\Big\langle \Psi_h^{n-l},\varrho\Big\rangle + (\Delta t)^{-\gamma}\sum_{l=0}^{n}\sigma_\gamma(l)\Big\langle \Upsilon_h^{n-l},\varrho\Big\rangle &= -(\Delta t)^{\alpha-1}\sum_{i=0}^{n}\varsigma_i^{\alpha-1}\mathcal{B}\Big\langle \Psi_h^{n-i},\varrho\Big\rangle \\ &\quad -\sum_{p=0}^{n} d_p\Big\langle \nabla\Psi_h^{n-p},\nabla\varrho\Big\rangle + \Big\langle \mathcal{R}_{\Delta t},\varrho\Big\rangle. \end{aligned}\tag{3.16}$$

Considering the value $\varrho = \Psi_h^n$ into the above equation, we have

$$\begin{aligned}(\Delta t)^{-\gamma}\sum_{l=0}^{n}\sigma_\gamma(l)\Big\langle \Psi_h^{n-l},\Psi_h^n\Big\rangle + (\Delta t)^{-\gamma}\sum_{l=0}^{n}\sigma_\gamma(l)\Big\langle \Upsilon_h^{n-l},\Psi_h^n\Big\rangle &= -(\Delta t)^{\alpha-1}\sum_{i=0}^{n}\varsigma_i^{\alpha-1}\mathcal{B}\Big\langle \Psi_h^{n-i},\Psi_h^n\Big\rangle \\ &\quad -\sum_{p=0}^{n} d_p\Big\langle \nabla\Psi_h^{n-p},\nabla\Psi_h^n\Big\rangle + \Big\langle \mathcal{R}_{\Delta t},\Psi_h^n\Big\rangle. \end{aligned}\tag{3.17}$$

By summing the above relation on the index n from $n = 0 : \mathcal{N}$, we get the following formula:

$$\begin{aligned}(\Delta t)^{-\gamma}\sum_{n=0}^{\mathcal{N}}\sum_{l=0}^{n}\sigma_\gamma(l)\Big\langle \Psi_h^{n-l},\Psi_h^n\Big\rangle + (\Delta t)^{-\gamma}\sum_{n=0}^{\mathcal{N}}\sum_{l=0}^{n}\sigma_\gamma(l)\Big\langle \Upsilon_h^{n-l},\Psi_h^n\Big\rangle &= -(\Delta t)^{\alpha-1}\sum_{n=0}^{\mathcal{N}}\sum_{i=0}^{n}\varsigma_i^{\alpha-1}\mathcal{B}\Big\langle \Psi_h^{n-i},\Psi_h^n\Big\rangle \\ &\quad -\sum_{n=0}^{\mathcal{N}}\sum_{p=0}^{n} d_p\Big\langle \nabla\Psi_h^{n-p},\nabla\Psi_h^n\Big\rangle + \sum_{n=0}^{\mathcal{N}}\Big\langle \mathcal{R}_{\Delta t},\Psi_h^n\Big\rangle. \end{aligned}\tag{3.18}$$

From the above equation, we have

$$\begin{aligned}&(\Delta t)^{-\gamma}\sum_{n=0}^{\mathcal{N}}\sum_{l=0}^{n}\sigma_\gamma(l)\Big\langle \Psi_h^{n-l},\Psi_h^n\Big\rangle \geq 0,\\ &\Psi_h^0 = 0,\\ &-\sum_{n=0}^{\mathcal{N}}\sum_{p=0}^{n} d_p\Big\langle \nabla\Psi_h^{n-p},\nabla\Psi_h^n\Big\rangle \leq 0. \end{aligned}\tag{3.19}$$

From Eq. (2.22), we get

$$(\Delta t)^{\alpha-1}\sum_{n=0}^{\mathcal{N}}\sum_{i=0}^{n}\varsigma_i^{\alpha-1}\mathcal{B}\Big\langle \Psi_h^n,\Psi_h^n\Big\rangle \geq (\Delta t)^{\alpha-1}\sum_{n=0}^{\mathcal{N}}\sum_{i=0}^{n}\varsigma_i^{\alpha-1}\mathcal{C}_5 \parallel \Psi_h^n \parallel^2_{\mathcal{H}^\vartheta(\Omega)\cap\mathcal{H}^\nu(\Omega)}. \tag{3.20}$$

Using Lemma 2.1, we have

$$\frac{(\Delta t)^{-\gamma}}{2}\sum_{n=0}^{\mathcal{N}}\sum_{l=0}^{n}\sigma_\gamma(l)\Big\langle \Psi_h^{n-i},\Psi_h^n\Big\rangle = \frac{(\Delta t)^{-\gamma}}{2}\Big(\sum_{n=0}^{\mathcal{N}}\parallel \Psi_h^n \parallel^2_{L^2(\Omega)}\sum_{l=0}^{n}\sigma_\gamma(l)\Big) < 0. \tag{3.21}$$

By applying Eqs. (3.19), (3.20) and (3.21), the equation (3.18) changes to the following relation

$$\frac{\gamma+2}{2}(\Delta t)^{-\gamma}\sum_{n=0}^{\mathcal{N}}\| \Psi_h^n \|^2_{L^2(\Omega)} + (\Delta t)^{\alpha-1}\sum_{n=0}^{\mathcal{N}}\sum_{i=0}^{n}\varsigma_i^{\alpha-1}\mathcal{C}_5\| \Psi_h^n \|^2_{\mathcal{H}^\vartheta(\Omega)\cap\mathcal{H}^\nu(\Omega)}$$
$$\leq \frac{(\Delta t)^{-\gamma}}{2}\sum_{n=0}^{\mathcal{N}}\sum_{l=0}^{n}\sigma_\gamma(l)\| \Upsilon_h^{n-l} \|^2_{L^2(\Omega)} + \frac{1}{4}\sum_{n=0}^{\mathcal{N}}\| \Psi_h^n \|^2_{L^2(\Omega)} + \sum_{n=0}^{\mathcal{N}}\| \mathcal{R}_{\Delta t} \|^2_{L^2(\Omega)}$$
$$+ \frac{1}{4}\sum_{n=0}^{\mathcal{N}}\| \Psi_h^n \|^2_{L^2(\Omega)}. \tag{3.22}$$

Also, we can be written Eq. (3.22) as

$$\sum_{j=0}^{\mathcal{N}}\| \Psi_h^j \|^2_{L^2(\Omega)} + 2(\Delta t)^{\alpha-1}\sum_{j=0}^{\mathcal{N}}\sum_{i=0}^{j}\varsigma_i^{\alpha-1}\mathcal{C}_5\| \Psi_h^j \|^2_{\mathcal{H}^\vartheta(\Omega)\cap\mathcal{H}^\nu(\Omega)}$$
$$\leq (\Delta t)^{-\gamma}\sum_{j=0}^{\mathcal{N}}\sum_{l=0}^{j}\sigma_\gamma(l)\| \Upsilon_h^{j-l} \|^2_{L^2(\Omega)} + 2\sum_{j=0}^{\mathcal{N}}\| \mathcal{R}_{\Delta t} \|^2_{L^2(\Omega)}. \tag{3.23}$$

Therefore, we can conclude from the above equation

$$\| \Psi_h^n \|^2_{L^2(\Omega)} \leq \sum_{j=0}^{\mathcal{N}}\| \Psi_h^j \|^2_{L^2(\Omega)} + 2(\Delta t)^{\alpha-1}\sum_{j=0}^{\mathcal{N}}\sum_{i=0}^{j}\varsigma_i^{\alpha-1}\mathcal{C}_5\| \Psi_h^j \|^2_{\mathcal{H}^\vartheta(\Omega)\cap\mathcal{H}^\nu(\Omega)}$$
$$\leq (\Delta t)^{-\gamma}\sum_{j=0}^{\mathcal{N}}\sum_{l=0}^{j}\sigma_\gamma(l)\| \Upsilon_h^{j-l} \|^2_{L^2(\Omega)} + 2\sum_{j=0}^{\mathcal{N}}\| \mathcal{R}_{\Delta t} \|^2_{L^2(\Omega)}. \tag{3.24}$$

Using Eq. (3.24) and Lemma 3.1, we obtain

$$\| \Psi_h^n \|^2_{L^2(\Omega)} \leq \mathcal{C}_8(\Delta t)^{-\gamma}(h^{\vartheta-\nu})^2\sum_{j=0}^{\mathcal{N}}\sum_{l=0}^{j}\sigma_\gamma(l) + 2\mathcal{C}_9\sum_{j=0}^{\mathcal{N}}(\Delta t)^{\frac{9}{4}}. \tag{3.25}$$

Then,

$$(\Delta t)^{\gamma}\| \Psi_h^n \|^2_{L^2(\Omega)} \leq 2\mathcal{C}_8\sum_{j=0}^{\mathcal{N}}(h^{\vartheta-\nu})^2 + 2\mathcal{C}_9(\Delta t)^{\gamma}\sum_{j=0}^{\mathcal{N}}(\Delta t)^{\frac{9}{4}}$$
$$\leq 2(\Delta t)^{\gamma}(\mathcal{C}_8+\mathcal{C}_9)\sum_{j=0}^{\mathcal{N}}\left((\Delta t)^{\frac{3}{2}} + h^{\vartheta-\nu}\right)^2$$
$$\leq \mathcal{C}_{10}\exp(T)\left((\Delta t)^{\frac{3}{2}} + h^{\vartheta-\nu}\right) \leq \mathcal{C}_7\left((\Delta t)^{\frac{3}{2}} + h^{\vartheta-\nu}\right). \tag{3.26}$$

Therefore, the proof of this theorem is concluded from the above equation. □

4. Numerical experiments

This part studies and checks the efficiency of the proposed numerical approach by analysing some numerical experiments along with simulation, from which we understand that the numerical approach has high accuracy compared to other methods. All numerical simulations were carried out using MATLAB software on a laptop equipped with an Intel Core i5 processor (2.40 GHz) and 16 GB of RAM. We state the computational order, which is presented by

$$Rate = \frac{\log_{10}\left(\frac{\mathcal{E}_1}{\mathcal{E}_2}\right)}{\log_{10}\left(\frac{h_1}{h_2}\right)}, \tag{4.1}$$

in which $\mathcal{E}_1$ and $\mathcal{E}_2$ are the absolute error function corresponding to steps h_1 and h_2, respectively.

Example 4.1. We consider the time-fractional model

$$\mathcal{D}_t^{\gamma} w(x,y,t) = \frac{1}{\Gamma(\alpha-1)} \int_0^t (t-\lambda)^{\alpha-2} \exp\big(-\upsilon(t-\lambda)\big)\Big(\frac{\partial^{\vartheta} w(x,y,\lambda)}{\partial |x|^{\vartheta}} + \frac{\partial^{\nu} w(x,y,\lambda)}{\partial |y|^{\nu}}\Big) d\lambda$$
$$+ \int_0^t \frac{1}{\sqrt{t-\tau}}\Big(\frac{\partial^2 w(x,y,\tau)}{\partial x^2} + \frac{\partial^2 w(x,y,\tau)}{\partial y^2}\Big) d\tau + h(x,y,t), \tag{4.2}$$

under the initial and boundary conditions

$$\begin{aligned} &w(x,y,0) = 0,\ (x,y) \in \Omega = (0,1)\times(0,1),\\ &w(x,y,t) = 0,\ (x,y) \in \partial\Omega,\ t \in (0,1), \end{aligned} \tag{4.3}$$

where $\mathbf{A}_y = \mathbf{A}_x = 1$ and

$$\begin{aligned} h(x,y,t) &= (x(1-x)y(1-y))^3 t^{4-\gamma}{}_1\Psi_1\left[\begin{matrix}(5,1)_{1,1}\\(5-\gamma,1)_{1,1}\end{matrix}\Big| -\upsilon t\right] - \frac{4!\exp\big(-\upsilon t\big)}{\Gamma(\alpha+4)}\\ &\times t^{\alpha+3}\Big\{v_1\big(y(1-y)\big)^3\big(\mathcal{Z}_1(x) - 3\mathcal{Z}_2(x)\\ &+ 3\mathcal{Z}_3(x) - \mathcal{Z}_4(x)\big) + v_2\big(x(1-x)\big)^3\big(\mathcal{T}_1(y) - 3\mathcal{T}_2(y) + 3\mathcal{T}_3(y) - \mathcal{T}_4(y)\big)\Big\}\\ &+ \sqrt{\pi} t^{\frac{9}{2}}{}_1\Psi_1\left[\begin{matrix}(5,1)_{1,1}\\(\frac{11}{2},1)_{1,1}\end{matrix}\Big| -\upsilon t\right]\Big\{6(x-x^2)^2 - 6(1-2x)^2(x-x^2) + 6(y-y^2)^2 - 6(1-2y)^2(y-y^2)\Big\}, \end{aligned} \tag{4.4}$$

in which $v_1 = -\Big(2\cos\big(\frac{\pi\vartheta}{2}\big)\Big)^{-1}$, $v_2 = -\Big(2\cos\big(\frac{\pi\nu}{2}\big)\Big)^{-1}$ and

$$\begin{aligned} &\mathcal{Z}_1(x) = \Gamma(4)\big(\Gamma(4-\vartheta)\big)^{-1}\big(x^{3-\vartheta} + (1-x)^{3-\vartheta}\big),\ \ \mathcal{Z}_2(x) = \Gamma(5)\big(\Gamma(5-\vartheta)\big)^{-1}\big(x^{4-\vartheta} + (1-x)^{4-\vartheta}\big),\\ &\mathcal{Z}_3(x) = \Gamma(6)\big(\Gamma(5-\vartheta)\big)^{-1}\big(x^{5-\vartheta} + (1-x)^{5-\vartheta}\big),\ \ \mathcal{Z}_4(x) = \Gamma(7)\big(\Gamma(6-\vartheta)\big)^{-1}\big(x^{6-\vartheta} + (1-x)^{6-\vartheta}\big),\\ &\mathcal{T}_1(y) = \Gamma(4)\big(\Gamma(4-\nu)\big)^{-1}\big(y^{3-\nu} + (1-y)^{3-\nu}\big),\ \ \mathcal{T}_2(y) = \Gamma(5)\big(\Gamma(5-\nu)\big)^{-1}\big(y^{4-\nu} + (1-y)^{4-\nu}\big),\\ &\mathcal{T}_3(y) = \Gamma(6)\big(\Gamma(5-\nu)\big)^{-1}\big(y^{5-\nu} + (1-y)^{5-\nu}\big),\ \ \mathcal{T}_4(y) = \Gamma(7)\big(\Gamma(6-\nu)\big)^{-1}\big(y^{6-\nu} + (1-y)^{6-\nu}\big). \end{aligned} \tag{4.5}$$

Here, the function ${}_p\Psi_q(t)$ shows the generalized Wright function and defined by [21, p. 184, 6.3.11] and [2] as follows:

$${}_p\Psi_q(t) = {}_p\Psi_q\left[\begin{matrix}(a_l,\alpha_l)_{1,p}\\(b_l,\beta_l)_{1,q}\end{matrix}\Big| t\right] = \sum_{k=0}^{\infty} \frac{\prod_{l=1}^{p}\Gamma(a_l+\alpha_l k)}{\prod_{j=1}^{q}\Gamma(b_j+\beta_j k)}\frac{t^k}{k!}. \tag{4.6}$$

The exact solution for this proposed model is $w(x,y,t) = t^4\exp\big(-\upsilon t\big)\big(xy(1-x)(1-y)\big)^3$. We solved the proposed model using the presented numerical approach and showed the numerical results in the form of graphs and tables. The parameters considered to obtain approximate solutions for the proposed model are $\vartheta = \nu = 1.75$, $\alpha = 1.5$, and $\upsilon = 0.1$ when $\mathcal{N} = 20$. Figure 1 shows the approximate solutions of the proposed model for the considered parameters using the presented numerical approach. The graph of the absolute error function is shown in Figure 2. Figure 3 shows the plot of the absolute error function with values $\vartheta = \nu = 1.75$, $\alpha = 1.5$, $\gamma = 0.95$, and $\upsilon = 0.1$ with various values of $\mathcal{N}$. A comparison between the computational orders and the absolute error function for different values of $\mathcal{N}$ when $\vartheta = \nu = 1.75$, $\alpha = 1.5$, and $\upsilon = 0.1$ is displayed in Table 1. From Table 1, we can see that when the time step becomes smaller, the value of the absolute error function decreases, and better approximations are obtained.

Example 4.2. We consider the time-fractional model

$$\mathcal{D}_t^{\gamma} w(x,y,t) = \frac{1}{\Gamma(\alpha-1)} \int_0^t (t-\lambda)^{\alpha-2} \exp\big(-\upsilon(t-\lambda)\big)\Big(\frac{\partial^{\vartheta} w(x,y,\lambda)}{\partial |x|^{\vartheta}} + \frac{\partial^{\nu} w(x,y,\lambda)}{\partial |y|^{\nu}}\Big) d\lambda$$
$$+ \int_0^t \frac{1}{\sqrt{t-\tau}}\Big(\frac{\partial^2 w(x,y,\tau)}{\partial x^2} + \frac{\partial^2 w(x,y,\tau)}{\partial y^2}\Big) d\tau, \tag{4.7}$$

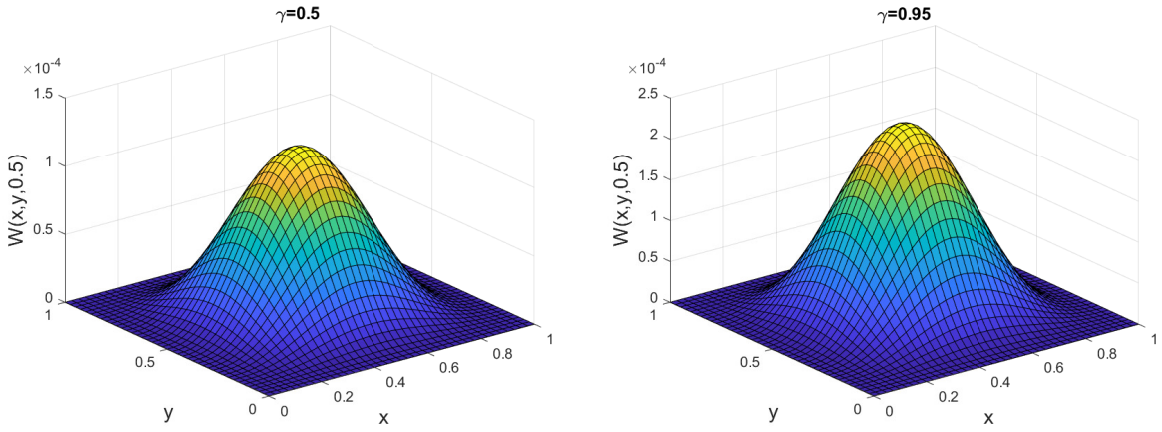

FIGURE 1. Plots of the approximate solutions with values $\vartheta = \nu = 1.75$, $\alpha = 1.5$, and $\upsilon = 0.1$ when $\mathcal{N} = 20$ for Example 4.1.

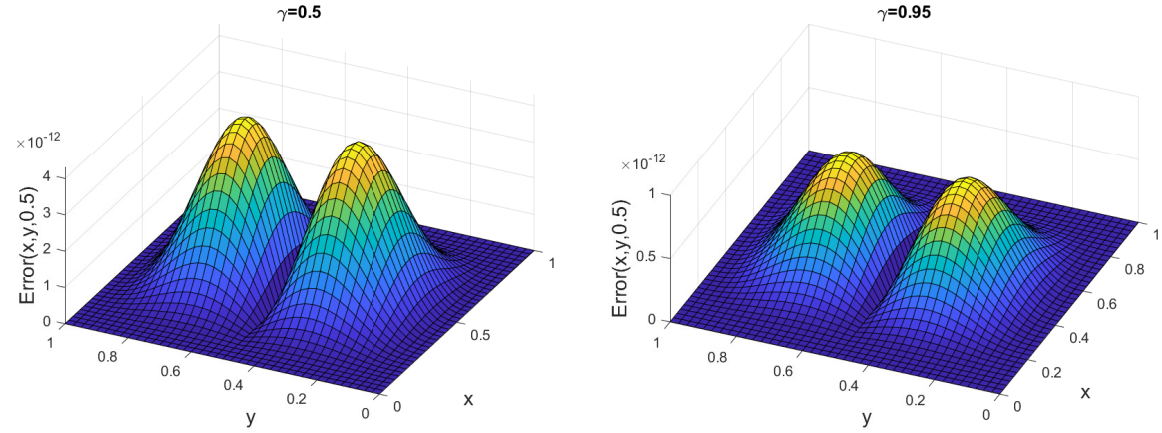

FIGURE 2. Plots of the absolute error function with values $\vartheta = \nu = 1.75$, $\alpha = 1.5$, and $\upsilon = 0.1$ when $\mathcal{N} = 20$ for Example 4.1.

under the initial and boundary conditions

$$\begin{aligned} &w(x,y,0) = \exp\big(-10\big\{(x-0.5)+(y-0.5)\big\}\big),\ (x,y) \in \Omega = (0,1)\times(0,1),\\ &w(x,y,t) = 0,\ (x,y) \in \partial\Omega,\ t \in (0,1), \end{aligned} \tag{4.8}$$

where $\mathbf{A}_y = \mathbf{A}_x = 1$. We solved this model using the proposed numerical approach for the values $\vartheta = \nu = 1.75$, $\alpha = 1.5$, and $\upsilon = 0.1$. To calculate and obtain the convergence order and approximate solutions using the suggested numerical approach, we follow the following steps:

1.: We consider a $\mathcal{N}^*$ and Δt that the value Δt is small enough and get the approximate solutions $W^{\Delta t}_{\mathcal{N}^*}$.

2.: Put $\mathcal{N}_1, \mathcal{N}_2, \ldots$ that $\mathcal{N}^* > \mathcal{N}^j$ for $j = 1, 2, \ldots$ and we get approximate solutions corresponding to the values $\mathcal{N}_1, \mathcal{N}_2, \ldots$ which are considered with $W^{\Delta t}_{\mathcal{N}_1}, W^{\Delta t}_{\mathcal{N}_2}, \ldots$.

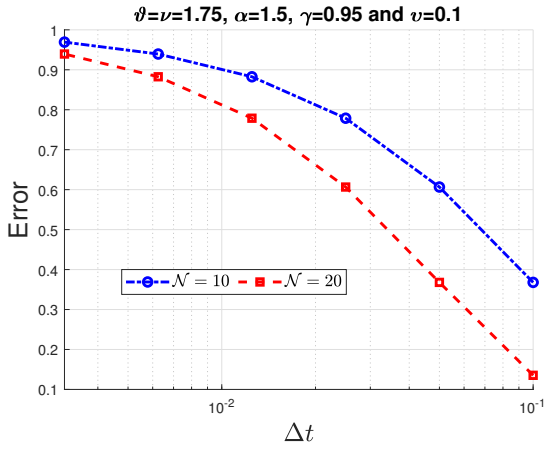

FIGURE 3. Plot of the absolute error function with values $\vartheta = \nu = 1.75$, $\alpha = 1.5$, $\gamma = 0.95$, and $\upsilon = 0.1$ with various values of $\mathcal{N}$ for Example 4.1.

TABLE 1. The comparison between the absolute error function, CPU time, and L_2 error for different values of $\mathcal{N}$ for Example 4.1 with $\vartheta = \nu = 1.75$, $\alpha = 1.5$, $\gamma = 0.95$, and $\upsilon = 0.1$.

Δt	$\mathcal{N}=10$		$\mathcal{N}=20$		$CPU-time$	L_2-Error	
	AE	Rate	AE	Rate		$\mathcal{N}=10$	$\mathcal{N}=20$
$\frac{1}{10}$	$5.5673e-14$	–	$1.1135e-14$	–	10	$1.23e-13$	$6.12e-14$
$\frac{1}{20}$	$2.7837e-14$	2.3020	$5.5673e-15$	2.0653	30	$6.78e-14$	$3.45e-14$
$\frac{1}{40}$	$1.3918e-14$	2.0730	$2.7837e-15$	2.0223	51	$3.45e-14$	$1.75e-14$
$\frac{1}{80}$	$6.9592e-15$	2.0107	$1.3918e-15$	2.0081	82	$1.75e-14$	$8.91e-15$
$\frac{1}{160}$	$3.4796e-15$	2.0053	$6.9592e-16$	2.0028	98	$8.91e-15$	$4.56e-15$
$\frac{1}{320}$	$1.7398e-15$	2.0011	$3.4796e-16$	2.0007	131	$4.34e-15$	$2.23e-15$

3.: Set

$$\mathrm{L}_{\infty}^{\mathcal{N}^*} = \max_{j=1,2,\ldots,\mathcal{M}-1} \left| W_{h^*}^{\Delta t} - W_{h^j}^{\Delta t} \right|, \; j = 1, 2, \ldots. \tag{4.9}$$

Numerical results for this proposed model are shown in Figures 4 and 5. Figure 4 shows the approximate solutions of the proposed model for the given values $\vartheta = \nu = 1.75$, $\alpha = 1.5$, and $\upsilon = 0.1$. A plot of the absolute error function is shown in Figure 5. The comparison between the error functions and computational orders is displayed in Tables 2 and 3 when $t = 0.5$. From Table 3, we can see that the convergence accuracy in the time variable direction using the proposed numerical approach is the second-order accuracy.

5. CONCLUSION

In this study, we have developed a high-performance, fully discrete numerical method to approximate solutions of the two-dimensional time-space diffusion-wave model with a weakly singular kernel in time and the Riesz fractional operator in space. By combining a second-order accurate difference scheme in time with a Galerkin spectral method based on generalized Jacobi functions in space, the proposed approach achieves both stability and second-order convergence accuracy in time. Numerical examples demonstrate the effectiveness and precision of the method, supported by comprehensive graphical and tabular results. While the proposed numerical method demonstrates robust accuracy and stability for the two-dimensional model, certain limitations should be acknowledged. Scalability to higher-dimensional or more complex systems may pose computational challenges due to the increased cost of the Galerkin spectral

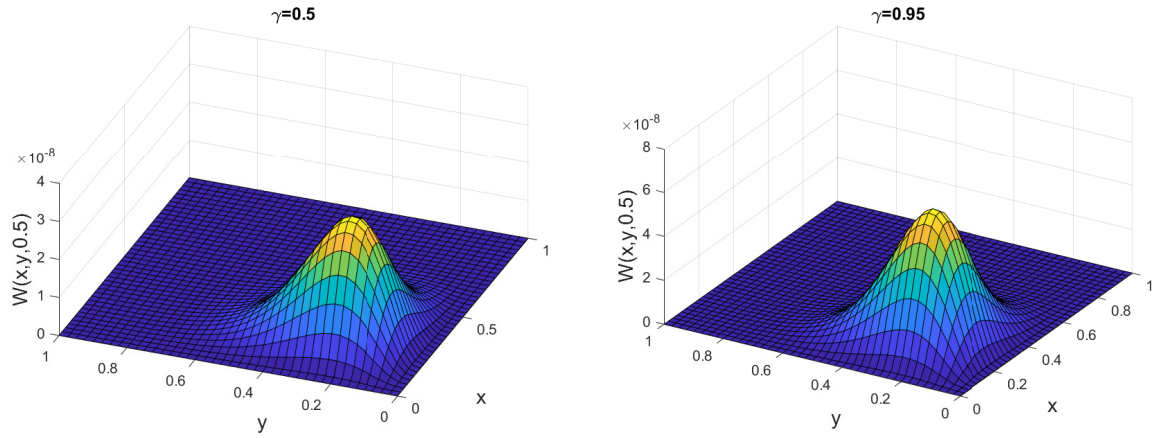

FIGURE 4. Plots of the approximate solutions with values $\vartheta = \nu = 1.75$, $\alpha = 1.5$, and $\upsilon = 0.1$ when $\mathcal{N} = 20$ for Example 4.2.

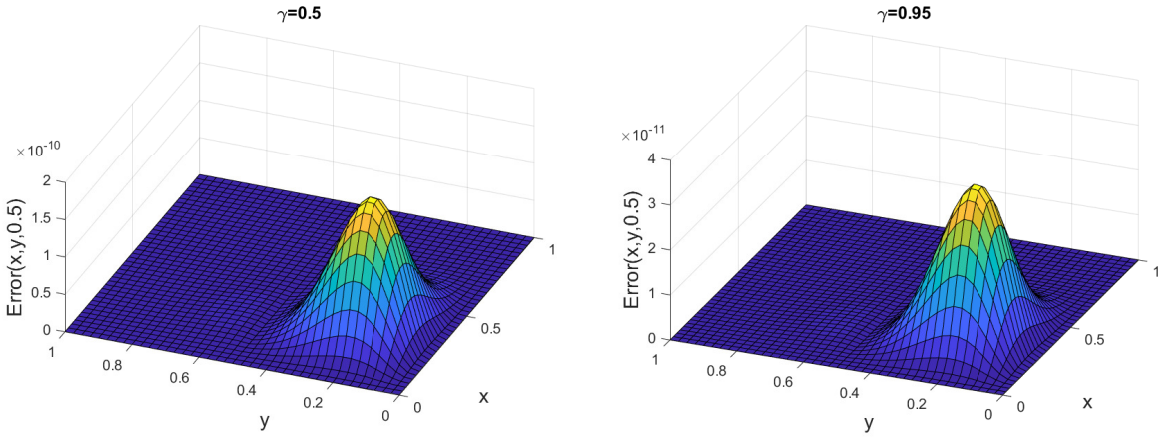

FIGURE 5. Plots of the absolute error function with values $\vartheta = \nu = 1.75$, $\alpha = 1.5$, and $\upsilon = 0.1$ when $\mathcal{N} = 20$ for Example 4.2.

method and the handling of fractional operators in multiple dimensions. Additionally, the current method assumes linearity and uniform discretization, which may limit its effectiveness in problems featuring nonlinear dynamics or highly irregular domains. Addressing these challenges will be essential to extend the applicability of the method to a wider range of practical problems. Despite these promising results, several avenues remain open for further investigation. Future work could extend the current framework to higher-dimensional models, enabling the analysis of more complex physical phenomena. Additionally, incorporating nonlinear terms into the diffusion-wave equation could provide a richer understanding of systems exhibiting nonlinear dynamics, requiring modifications to the numerical scheme. Improving computational efficiency through adaptive mesh refinement techniques presents another important direction, particularly in handling regions with steep solution gradients or singular behavior. Implementing parallel computing strategies could further enhance the scalability of the method for large-scale simulations.

Data availability statement. All data that support the findings of this study are included within the article.

TABLE 2. The comparison between the absolute error function, CPU time, and computational orders for Example 4.2 with values of $\vartheta = \nu = 1.75$, $\alpha = 1.5$, $\gamma = 0.95$, and $\upsilon = 0.1$.

$\mathcal{N}$	$\mathcal{N}^* = 80,\ \Delta t = \frac{1}{1000}$		$\mathcal{N}^* = 80,\ \Delta t = \frac{1}{100000}$		$CPU - time$
	$L_\infty^{\mathcal{N}^*}$	$Rate$	$L_\infty^{\mathcal{N}^*}$	$Rate$	
5	$6.4546e-14$	–	$1.2909e-15$	–	16
10	$3.2273e-14$	5.7046	$6.4546e-16$	5.7008	76
20	$1.6136e-14$	6.1843	$3.2273e-16$	7.7023	136
30	$1.0758e-14$	7.6517	$2.1515e-16$	8.5702	246
40	$8.0682e-15$	8.4109	$1.6136e-16$	11.6550	393

TABLE 3. The comparison between the absolute error function and computational orders for Example 4.2 with values of $\vartheta = \nu = 1.75$, $\alpha = 1.5$, $\gamma = 0.95$, and $\upsilon = 0.1$.

Δt	$\mathcal{N}^* = 40,\ \Delta t = \frac{1}{10000}$		$\mathcal{N}^* = 80,\ \Delta t = \frac{1}{10000}$	
	AE	$Rate$	AE	$Rate$
$\frac{1}{10}$	$3.2273e-14$	–	$6.4546e-14$	–
$\frac{1}{20}$	$1.6136e-14$	1.9941	$3.2273e-14$	1.9933
$\frac{1}{40}$	$8.0682e-15$	1.9995	$1.6136e-14$	1.9911
$\frac{1}{80}$	$4.0341e-15$	1.9998	$8.0682e-15$	1.9988
$\frac{1}{160}$	$2.0171e-15$	1.9999	$4.0341e-15$	1.9991

Funding. NA

Competing interests. The authors have no relevant financial or non-financial interests to disclose.

REFERENCES

[1] W. M. Abd-Elhameed and Y. H. Youssri, *Fifth-kind orthonormal Chebyshev polynomial solutions for fractional differential equations*, Computational and Applied Mathematics, *37* (2018), 2897–2921.

[2] A. Ansari, M. H. Derakhshan, and H. Askari, *Distributed order fractional diffusion equation with fractional Laplacian in axisymmetric cylindrical configuration*, Communications in Nonlinear Science and Numerical Simulation, *113* (2022), 106590.

[3] M. Abbaszadeh, M. Dehghan, and Y. Zhou, *Crank–Nicolson/Galerkin spectral method for solving two-dimensional time-space distributed-order weakly singular integro-partial differential equation*, Journal of Computational and Applied Mathematics, *374* (2020), 112739.

[4] L. An and L. Ling, *The Riemann–Hilbert approach for the integrable fractional Fokas–Lenells equation*, Studies in Applied Mathematics, *152*(4) (2024), 1177–1207.

[5] A. H. Bhrawy and M. A. Zaky, *Numerical simulation of multi-dimensional distributed-order generalized Schrödinger equations*, Nonlinear Dynamics, *89* (2017), 1415–1432.

[6] W. Bu, Y. Tang, Y. Wu, and J. Yang, *Finite difference/finite element method for two-dimensional space and time fractional Bloch–Torrey equations*, Journal of Computational Physics, *293* (2015), 264–279.

[7] H. Borluk, G. Bruell, and D. Nilsson, *Traveling waves and transverse instability for the fractional Kadomtsev–Petviashvili equation*, Studies in Applied Mathematics, *149*(1) (2022), 95–123.

[8] A. Bueno-Orovio and K. Burrage, *Exact solutions to the fractional time-space Bloch–Torrey equation for magnetic resonance imaging*, Communications in Nonlinear Science and Numerical Simulation, *52* (2017), 91–109.

[9] M. Chen and W. Deng, *Discretized fractional substantial calculus*, ESAIM: Mathematical Modelling and Numerical Analysis, *49*(2) (2015), 373–394.

[10] R. Cai, S. Kosari, J. Shafi, and M. H. Derakhshan, *Stability analysis study for the time-fractional Galilei invariant advection-diffusion model of distributive order using an efficient hybrid approach*, Physica Scripta, *99*(12) (2024), 125229.

[11] M. H. Derakhshan, H. Rezaei, and H. R. Marasi, *An efficient numerical method for the distributed order time-fractional diffusion equation with error analysis and stability*, Mathematics and Computers in Simulation, *214* (2023), 315–333.
[12] M. H. Derakhshan and Y. Ordokhani, *Numerical and stability analysis of linear B-spline and local radial basis functions for solving two-dimensional distributed-order time-fractional telegraph models*, Journal of Applied Mathematics and Computing, (2025), 1–29.
[13] M. H. Derakhshan, S.L. Mortazavifar, P. Veeresha, and J. F. Gómez-Aguilar, *An efficient hybrid approach for numerical study of two-dimensional time-fractional Cattaneo model with Riesz distributed-order space-fractional operator along with stability analysis*, Physica Scripta, *99*(9) (2024), 095242.
[14] M. H. Derakhshan, P. Kumar, and S. Salahshour, *A high-order space-time spectral method for the distributed-order time-fractional telegraph equation*, International Journal of Dynamics and Control, (2024), 1–17.
[15] M. H. Derakhshan, A. Ansari, and M. R. Ahmadi Darani, *On asymptotic stability of Weber fractional differential systems*, Computational Methods for Differential Equations, *6*(1) (2018), 30–39.
[16] M. H. Derakhshan and A. Ansari, *Numerical approximation to Prabhakar fractional Sturm–Liouville problem*, Computational and Applied Mathematics, *38*(2) (2019), 71.
[17] Q. Ding, X. Long, and S. Mao, *Convergence analysis of Crank-Nicolson extrapolated fully discrete scheme for thermally coupled incompressible magnetohydrodynamic system*, Applied Numerical Mathematics, *157* (2020), 522–543.
[18] H. Du, Z. Chen, and T. Yang, *A stable least residue method in reproducing kernel space for solving a nonlinear fractional integro-differential equation with a weakly singular kernel*, Applied Numerical Mathematics, *157* (2020), 210–222.
[19] M. H. Derakhshan, H. R. Marasi, and P. Kumar, *A linear B-spline interpolation/Galerkin finite element method for the two-dimensional Riesz space distributed-order diffusion-wave equation with error analysis*, The European Physical Journal Plus, *139*(4) (2024), 1–17.
[20] K. Diethelm, N. J. Ford, and A. D. Freed, *Detailed error analysis for a fractional Adams method*, Numerical Algorithms, *36*(1) (2004), 31–52.
[21] R. Gorenflo, A. A. Kilbas, F. Mainardi, and S. Rogosin, *Mittag-Leffler Functions, Related Topics and Applications*, Springer, Berlin, 2020.
[22] X. M. Gu and S. L. Wu, *A parallel-in-time iterative algorithm for Volterra partial integro-differential problems with weakly singular kernel*, Journal of Computational Physics, *417* (2020), 109576.
[23] B. Ghosh and J. Mohapatra, *Analysis of a second-order numerical scheme for time-fractional partial integro–differential equations with a weakly singular kernel*, Journal of Computational Science, *74* (2023), 102157.
[24] M. Hamid, T. Zubair, M. Usman, and R. U. Haq, *Numerical investigation of fractional-order unsteady natural convective radiating flow of nanofluid in a vertical channel*, AIMS Math, *4*(5) (2019), 1416–1429.
[25] S. Irandoust-Pakchin, M. H. Derakhshan, S. Rezapour, and M. Adel, *An efficient numerical method for the distributed-order time-fractional diffusion equation with the error analysis and stability properties*, Mathematical Methods in the Applied Sciences, *48*(3) (2025), 2743–2765.
[26] S. Kosari, P. Xu, J. Shafi, and M. H. Derakhshan, *An efficient hybrid numerical approach for solving two-dimensional fractional cable model involving time-fractional operator of distributed order with error analysis*, Numerical Algorithms, (2024), 1–20.
[27] Y. Luchko, *Fractional wave equation and damped waves*, Journal of Mathematical Physics, *54*(3) (2013), 031505.
[28] Z. Liu, F. Liu, and F. Zeng, *An alternating direction implicit spectral method for solving two dimensional multi-term time fractional mixed diffusion and diffusion-wave equations*, Applied Numerical Mathematics, *136* (2019), 139–151.
[29] M. Lakestani and J. Manafian, *Analytical treatments of the space–time fractional coupled nonlinear Schrödinger equations*, Optical and Quantum Electronics, *50* (2018), 1–33.
[30] J. Li, F. Liu, L. Feng, and I. Turner, *A novel finite volume method for the Riesz space distributed-order advection–diffusion equation*, Applied Mathematical Modelling, *46* (2017), 536–553.

[31] N. Moshtaghi and A. Saadatmandi, *Numerical solution of time fractional cable equation via the sinc-Bernoulli collocation method*, Journal of Applied and Computational Mechanics, *7*(4) (2021), 1916–1924.
[32] J. Manafian and M. Lakestani, *Interaction among a lump, periodic waves, and kink solutions to the fractional generalized CBS-BK equation*, Mathematical Methods in the Applied Sciences, *44*(1) (2021), 1052–1070.
[33] R. Metzler and J. Klafter, *The random walk's guide to anomalous diffusion: a fractional dynamics approach*, Physics Reports, *339*(1) (2000), 1–77.
[34] F. Mainardi, G. Pagnini, and R. Gorenflo, *Some aspects of fractional diffusion equations of single and distributed order*, Applied Mathematics and Computation, *187*(1) (2007), 295–305.
[35] H. R. Marasi, M. H. Derakhshan, A.A. Ghuraibawi, and P. Kumar, *A novel method based on fractional order Gegenbauer wavelet operational matrix for the solutions of the multi-term time-fractional telegraph equation of distributed order*, Mathematics and Computers in Simulation, *217*(2024), 405–424.
[36] Z. Mao and G. E. Karniadakis, *A spectral method (of exponential convergence) for singular solutions of the diffusion equation with general two-sided fractional derivative*, SIAM Journal on Numerical Analysis, *56*(1) (2018), 24–49.
[37] F. Mainardi and G. Spada, *Creep, relaxation and viscosity properties for basic fractional models in rheology*, The European Physical Journal Special Topics, *193*(1) (2011), 133–160.
[38] A. Quarteroni and A. Valli, *Numerical Approximation of Partial Differential Equations*, Springer-Verlag, New York, 1997.
[39] P. Rahimkhani and M. H. Heydari, *Numerical investigation of Ψ-fractional differential equations using wavelets neural networks*, Computational and Applied Mathematics, *44*(1) (2025), 54.
[40] A. Safaei, A. H. Salehi Shayegan, and M. Shahriari, *Two-dimensional temporal fractional advection-diffusion problem resolved through the Sinc-Galerkin method*, Computational Methods for Differential Equations, (2024).
[41] S. Shamseldeen, A. Elsaid, and S. Madkour, *Caputo–Riesz-Feller fractional wave equation: analytic and approximate solutions and their continuation*, Journal of Applied Mathematics and Computing, *59* (2019), 423–444.
[42] W. Tian, H. Zhou, and W. Deng, *A class of second order difference approximations for solving space fractional diffusion equations*, Mathematics of Computation, *84*(294) (2015), 1703–1727.
[43] T. Tang, *A finite difference scheme for a partial integro–differential equations with a weakly singular kernel*, Applied Numerical Mathematics, *11* (1993), 309–319.
[44] F. Wang, X. Yang, H. Zhang, and L. Wu, *A time two-grid algorithm for the two dimensional nonlinear fractional PIDE with a weakly singular kernel*, Mathematics and Computers in Simulation, *199* (2022), 38–59.
[45] Z. Yang, F. Liu, Y. Nie, and I. Turner, *An unstructured mesh finite difference/finite element method for the three-dimensional time-space fractional Bloch-Torrey equations on irregular domains*, Journal of Computational Physics, *408* (2020), 109284.
[46] P. Zhuang, F. Liu, I. Turner, and Y. T. Gu, *Finite volume and finite element methods for solving a one-dimensional space-fractional Boussinesq equation*, Applied Mathematical Modelling, *38*(15–16) (2014), 3860–3870.
[47] R. Zheng, F. Liu, X. Jiang, and I. W. Turner, *Finite difference/spectral methods for the two-dimensional distributed-order time-fractional cable equation*, Computers & Mathematics with Applications, *80*(6) (2020), 1523–1537.
[48] F. Zeng, F. Liu, C. Li, K. Burrage, I. Turner, and V. Anh, *A Crank–Nicolson ADI spectral method for a two-dimensional Riesz space fractional nonlinear reaction-diffusion equation*, SIAM Journal on Numerical Analysis, *52*(6) (2014), 2599–2622.